Design of P1′ and P3′ Residues of Trivalent Thrombin Inhibitors and Their Crystal Structures†

Jacek J. Slon-Usakiewicz, J. Sivaraman, Yunge Li, Miroslaw Cygler, and Yasuo Konishi*

Biotechnology Research Institute, National Research Council of Canada, 6100 Royalmount Avenue, Montreal, Quebec H4P 2R2, Canada

Received October 18, 1999; Revised Manuscript Received December 14, 1999

ABSTRACT: Synthetic bivalent thrombin inhibitors comprise an active site blocking segment, a fibrinogen recognition exosite blocking segment, and a linker connecting these segments. Possible nonpolar interactions of the P1′ and P3′ residues of the linker with thrombin S1′ and S3′ subsites, respectively, were identified using the "Methyl Scan" method [Slon-Usakiewicz et al. (1997) *Biochemistry 36,* 13494−13502]. A series of inhibitors (4-*tert*-butylbenzenesulfonyl)-Arg-(D-pipecolic acid)-Xaa-Gly-Yaa-Gly-βAla-Asp-Tyr-Glu-Pro-Ile-Pro-Glu-Glu-Ala-(β-cyclohexylalanine)-(D-Glu)-OH, in which nonpolar P1′ residue Xaa or P3′ residue Yaa was incorporated, were designed and improved the affinity to thrombin. Substitution of the P3′ residue with D-phenylglycine or D-Phe improved the K_i value to $(9.5 \pm 0.6) \times 10^{-14}$ or $1.3 \pm 0.5 \times 10^{-13}$ M, respectively, compared to that of a reference inhibitor with Gly residues at Xaa and Yaa residues ($K_i = (2.4 \pm 0.5) \times 10^{-11}$ M). Similarly, substitution of the P1′ residue with L-norleucine or L-β-(2-thienyl)alanine lowered the K_i values to $(8.2 \pm 0.6) \times 10^{-14}$ or $(5.1 \pm 0.4) \times 10^{-14}$ M, respectively. The linker Gly-Gly-Gly-βAla of the inhibitors in the previous sentence was simplified with 12-aminododecanoic acid, resulting in further improvment of the K_i values to $(3.8 \pm 0.6) \times 10^{-14}$ or $(1.7 \pm 0.4) \times 10^{-14}$ M, respectively. These K_i values are equivalent to that of natural hirudin (2.2×10^{-14} M), yet the size of the synthetic inhibitors (2 kD) is only one-third that of hirudin (7 kD). Two inhibitors, with L-norleucine or L-β-(2-thienyl)alanine at the P1′ residue and the improved linker of 12-aminododecanoic acid, were crystallized in complex with human α-thrombin. The crystal structures of these complexes were solved and refined to 2.1 Å resolution. The Lys^{60F} side chain of thrombin moved significantly and formed a large nonpolar S1′ subsite to accommodate the bulky P1′ residue.

Thrombin is a proteolytic regulatory enzyme of coagulation cascade. Upon vascular injury, thrombin is activated from prothrombin and converts soluble fibrinogen into insoluble fibrin clot. Thrombin also hydrolyzes the amide bonds of protein C and thrombin receptor on the platelet surface. The new N-terminal sequences generated by hydrolysis of various substrates have been shown in several cases to have specific biological functions. For example, after release of fibrinopeptide A, the newly formed N-terminal Gly-Pro-Arg-Val- sequence of fibrin binds to the C-terminal domain of other fibrin molecules to form fibrin clot (*1*).[1] The newly formed N-terminal Ser^{42}-Phe-Leu-Leu-Arg-... of the thrombin receptor after cleaving at the Arg^{41}-Ser^{42} bond binds intramolecularly and activates the receptors of human platelets and vascular endothelial cells (*2*). Thus, the sequence of P′ residues has dual functions, as a substrate and as a functional site of the cleaved protein.

Thrombin cleaves proteins at a limited number of sites. The primary specificity of thrombin is determined by P1 residue Arg/Lys due to an ionic interaction with Asp^{189} at the bottom of the S1 subsite.[2,3] However, thrombin cleaves only four Arg-Gly bonds among 376 Arg/Lys-Xaa bonds in fibrinogen to release fibrinopeptides (*5*). The high specificity is thus arrived from other interactions. The S2 subsite of thrombin is nonpolar, and Pro is by far the preferred P2 residue (*6*). The S3 subsite of thrombin is called "the aryl binding site" and prefers aromatic or nonpolar amino acids, e.g., Phe^{8} and Leu^{9} of fibrinogen, to occupy the S3 subsite (*7*). Thrombin also has unique insertion loops B (Tyr^{60A}-Ile^{60I}) and C (Thr^{149A}-Ala^{149E}), contributing to the substrate specificity. Especially, it has been pointed out that the Lys^{60F} side chain excludes bulky amino acids of the P1′ residue (*4*). For example, a mutagenesis of Lys^{60F} with Ala enhanced the affinity of the bulky Leu P1′ residue (*8*). The P2′ residue in natural substrates and inhibitors of thrombin is very diverse, e.g., Phe, Leu, Val, Ile, Pro, Gly, His, Glu, and Asn; however, k_{cat}/K_m of synthetic substrates showed a preference for bulky hydrophobic P2′ residues such as Phe and Trp,

† NRCC Publication No. 42940.

* To whom correspondence should be addressed. Phone: (514) 496-6339. Fax: (514) 496-5143. E-mail: Yasuo.Konishi@nrc.ca.

[1] Amino acids used in this paper are in the L-configuration unless specified as D-amino acid for D-isomer and D,L for racemic mixture.

[2] The substrate/inhibitor and subsite nomenclature was suggested by Schechter and Berger (*3*) such that residues of substrates/inhibitors were numbered P1, P2, P3, etc., toward the amino terminus from the scissile peptide bond, and the complementary subsites of the enzyme were numbered S1, S2, S3, etc., respectively. The residues of some inhibitors such as MD-805, NAPAP, and TAPAP are exceptionally numbered as P3, P1, and P2 from the N-terminus, reflecting their occupations of thrombin S3, S1, and S2 subsites, respectively, in the complex.

[3] The numbering of human α-thrombin residues is based on the chymotrypsin sequence (*4*).

10.1021/bi992419b CCC: $19.00
Published on Web 02/10/2000

whereas acidic amino acids of Glu and Asp were not favored (*6*). Similarly, the P3′ residue in natural substrates and inhibitors of thrombin is very diverse, e.g., Arg, Asn, His, Leu, Gly, and Asp; however, k_{cat}/K_m of synthetic substrates showed a preference for basic and bulky hydrophobic amino acid as the P3′ residue, whereas acidic amino acids of Glu and Asp were not favored (*6*). Indeed, protein C, having Asp at the P3′ residue, is a poor substrate of thrombin, and is actively hydrolyzed only when the substrate specificity of thrombin is changed by the binding of thrombomodulin. The S′ subsites of thrombin form a long and deep cleft toward the FRE.[4] The physiological function of this cleft is not well understood.

Bivalent thrombin inhibitors bind to the active site and the FRE of thrombin simultaneously, and a linker connects these two blocking segments. Three types of bivalent inhibitors have been developed. The first type of inhibitor is a (substrate-type active site inhibitor segment [e.g., (D-Phe)^{H1}-Pro^{H2}-Arg^{H3}-Pro^{H4}])-(linker)-(FRE inhibitor segment [e.g., hirudin$^{55-65}$]) (*9*−*11*).[5] Since the scissile bond at Arg^{H3}-Pro^{H4} is slowly hydrolyzed by thrombin, various pseudopeptide bonds or transition-state analogues have been developed. However, the synthesis of the pseudopeptide bonds or transition-state analogues may require tedious organic chemistry with low yield (*12*−*15*). Inhibitors of the second type mimic the binding mode of hirudin with a typical sequence of (P1-P2-P3 or P2-P1-P3)-(linker)-(FRE inhibitor segment) (*16*−*18*). The active site inhibitor segment binds in reverse to the substrates, and a long linker bridges between the P3 residue and the N-terminal Asp^{H55} of the FRE inhibitor segment. These inhibitors advantageously avoid the scissile bond or are able to incorporate transition-state analogues. This arrangement eliminated the N-terminal free amino group of the P3 residue, which, in the substrate-type inhibitor segment, enhanced the affinity ~100-fold (*19*). Thus, the affinity of inhibitors of this type could be only <10-fold better than the corresponding active site inhibitors (*17*). Inhibitors of the third type utilize high affinity of nonsubstrate-type inhibitors such as MD-805 and NAPAP (*20*). The scissile bond is eliminated by connecting the P1′ residue directly to the P2 residue. Tsuda et al. (*20*) successfully designed this class of inhibitors with K_i values on the order of 10^{-11} M. The inhibitors were synthesized by using conventional SPPS with ~70% purity in the crude products. The inhibitors also made it possible to design the linker as P′ residues for additional interactions with thrombin since short linkers lie along the deep cleft at the S′ subsites. Nonpolar interactions were searched for using a "Methyl Scan" in which a methyl side chain was introduced at each backbone atom of the linker and the K_i values of the inhibitors were evaluated (*21*). The methyl side chain at the second and eighth atoms of the 16-atom linker, corresponding to the P1′ and P3′ residues, respectively, improved the affinity of the inhibitor by 20−25-fold with L- and D-configurations, respectively.[6] This was rather contradictory to the strong preference for small amino acids as the P1′ residue. The preference for nonpolar D-amino acids at the P3′ residue was novel since no D-amino acids had been studied.

In this paper a series of inhibitors, Bbs-Arg-(D-Pip)-Xaa-Gly-Yaa-Gly-βAla-Asp-Tyr-Glu-Pro-Ile-Pro-Glu-Glu-Ala-Cha-(D-Glu)-OH, were used, where Xaa and Yaa are Gly or various D- or L-nonpolar amino acids. The crystal structures of two inhibitors in complex with thrombin are presented.

EXPERIMENTAL PROCEDURES

Materials. Human α-thrombin (3000 NIH units/mg) for enzymatic assay, bovine fibrinogen (70% protein, 85% of protein clottable), Tos-Gly-Pro-Arg-AMC·HCl salt, poly(ethylene glycol) 8000, and Tris were purchased from Sigma (St. Louis, MO). Human α-thrombin for crystallization was purchased from Haematologic Technologies Inc. (Essex Junction, VT) and was used without further purification. All Fmoc-amino acids and all other amino acid derivatives for peptide synthesis were purchased from Advanced ChemTech (Louisville, KY), Bachem Bioscience Inc. (King of Prussia, PA), and Calbiochem-Novabiochem (San Diego, CA). Fmoc-D-Glu(OtBu)-Wang resin (0.59 mmol/g) was purchased from Calbiochem-Novabiochem. The solvents for peptide synthesis were obtained from B&J Chemicals (Muskegon, MI) and Perkin-Elmer/Applied Biosystems (Foster City, CA). Citric acid, diethyl ether, and glacial acetic acid were purchased from Anachemia Chemical Inc. (Rouses Point, NY). TFA was purchased from Halocarbon Products Co. (River Edge, NJ). Phenol, thioaninsole, potassium sulfate, sodium phosphate, and ethanedithiol were purchased from Aldrich (Milwaukee, WI).

Peptide Synthesis. The peptides were synthesized by using the solid-phase method on a 396 multiple peptide synthesizer (Advanced ChemTech) using a conventional Fmoc procedure. Peptides were cleaved from the resin using Reagent K (TFA (82.5%)/water(5%)/phenol (5%)/thioanisole (5%)/ethanedithiol (2.5%); 25 mL/g peptide-resin) for 2−4 h at room temperature. After precipitation with diethyl ether, peptides were filtered, dissolved in 50% acetic acid, and lyophilized. The peptides were then purified by a preparative HPLC (Vydac C_4 column, 4.6 × 25 cm) using a linear gradient of 20−50% acetonitrile in 0.1% TFA (0.5%/min gradient; 33 mL/min flow rate). The final products were lyophilized with 98% or higher purity estimated by an analytical HPLC (Vydac C_{18} column, 0.46 × 25 cm; 10−60% acetonitrile in 0.1% TFA; 1.0%/min gradient; 1.0 mL/

[4] Abbreviations: αAbu, α-aminobutyric acid; βAla, β-alanine; λAdod, 12-aminododecanoic acid; αAib, α-aminoisobutyric acid; AMC, 7-amino-4-methylcoumarin; Bbs, 4-*tert*-butylbenzenesulfonyl; Cha, β-cyclohexylalanine; Chg, cyclohexylglycine; Fmoc, 9-fluorenylmethoxycarbonyl; FRE, fibrinogen recognition exo site; Hph, homophenylalanine; HPLC, high-performance liquid chromatography; MD-805, (2*R*,4*R*)-4-methyl-1-[*N*α-(3-methyl-1,2,3,4-tetrahydro-8-quinolinesulfonyl)-L-arginyl]-2-piperidinecarboxylic acid; NAPAP, *N*α-(2-naphthylsulfonylglycyl)-D,L-*p*-amidinophenylalanylpiperidine; Nle, norleucine; Nva, norvaline; Pen, β,β-dimethylcysteine; Phg, phenylglycine; Pip, pipecolic acid; SPPS, solid-phase peptide synthesis; Tbg, *tert*-butylglycine; TFA, trifluoroacetic acid; Thi, β-(2-thienyl)alanine; Tos, *p*-toluenesulfonyl; Tris, 2-amino-2-(hydroxymethyl)-1,3-propanediol.

[5] The numbering of the inhibitor residues is based on the hirudin sequence, and "H" is added to the residue number of the inhibitors, e.g., Bbs^{H1}-Arg^{H2}-(D-Pip)^{H3}-Gly^{H4}-Gly^{H5}-Gly^{H6}-Gly^{H7}-βAla^{H8}-Asp^{H55}-Tyr^{H56}-Glu^{H57}-Pro^{H58}-Ile^{H59}-Pro^{H60}-Glu^{H61}-Glu^{H62}-Ala^{H63}-Cha^{H64}-(D-Glu)^{H65}-OH.

[6] The linkers were named according to the number of atoms contributing to the length of the linkers; e.g., a linker 4-aminobutyric acid is a 5-atom linker and (12-aminododecanoic acid−4-aminobutyric acid) is an 18-atom linker. For convenience, in this paper, the P1′ moiety of the linker is connected to the P2 residue and marks the start of the linker. This differs from the previous numbering scheme where the linker began after the P1′ residue (*22*).

min flow rate). The elution profile was monitored by an absorbance at 210 and 254 nm for the analytical HPLC, and 220 nm for the preparative HPLC. The peptides were identified with a Beckman model 6300 amino acid analyzer (Beckman, Fullerton, CA) and an API III mass spectrometer (Sciex, Concord, Ontario, Canada). Amino acid analysis was used for peptide content determination. All peptides used in this paper have correct amino acid compositions and molecular masses.

Amidolytic Assays. The inhibition of amidolytic activity of human α-thrombin was measured fluorometrically using Tos-Gly-Pro-Arg-AMC as a fluorogenic substrate in 50 mM Tris·HCl buffer (pH 7.80 at 25 °C) containing 0.1 M NaCl and 0.1% poly(ethylene glycol) 8000 at room temperature (*23*). The final concentrations of the inhibitors, the substrate, and human α-thrombin were $(0.5-1000)K_i$, $(1-8) \times 10^{-6}$ M, and 3.0×10^{-11} M, respectively, if $K_i > 10^{-10}$ M; $(10-100)K_i$, $(5-40) \times 10^{-6}$ M, and 3.0×10^{-11} M, respectively, if 10^{-10} M $> K_i > 10^{-11}$ M; and $(3.3-56) \times 10^{-10}$, $(5-40) \times 10^{-6}$, and 3.0×10^{-11} M, respectively, if $K_i < 10^{-11}$ M. The hydrolysis of the substrate by thrombin was monitored on a Hitachi F2000 fluorescence spectrophotometer and a Parkin-Elmer LS50B luminescence spectrophotometer ($\lambda_{ex} = 383$ nm; $\lambda_{em} = 455$ nm), and the fluorescent intensity was calibrated by using AMC. The substrate and an inhibitor were premixed at appropriate concentrations (the solution volume was adjusted to 2.99 mL) before 10 μL of human α-thrombin (9×10^{-9} M) was added. The reaction reached a steady state within 3 min after the hydrolysis started. The steady-state velocity was then measured for a few minutes. The kinetic data of the steady-state velocity at various concentrations of the substrate and the inhibitors of the competitive inhibition were analyzed using the methods described in refs *22* and *24*. Microsoft Excel was used to estimate the kinetic parameters (K_m, V_{max}, and K_i).

Crystallization and Data Collection. Two thrombin inhibitors, P628 [Bbs-Arg-(D-Pip)-Nle-λAdod-Asp-Tyr-Glu-Pro-Ile-Pro-Glu-Glu-Ala-Cha-(D-Glu)-OH] and P798 [Bbs-Arg-(D-Pip)-Thi-λAdod-Asp-Tyr-Glu-Pro-Ile-Pro-Glu-Glu-Ala-Cha-(D-Glu)-OH], were cystallized in complex with human α-thrombin. The thrombin−inhibitor complexes were prepared by overnight incubation of thrombin (6 mg/mL) with inhibitor P628 or P798 at a molar ratio of 1:2 in 50 mM potassium sulfate, 50 mM citrate buffer (pH 5.5) at 4 °C. The crystals were grown by using the hanging drop vapor diffusion method with a reservoir solution of 25% (w/v) poly(ethylene glycol) 4000, 40 mM potassium sulfate, and 100 mM citric acid buffered to pH 5.5 with sodium phosphate at 18 °C. The pH of the reservoir solution was adjusted. The crystallization drops contained 2 μL of thrombin−inhibitor complex solution and 4 μL of the reservoir solution. Rodlike crystals were harvested after 3−4 days. Diffraction data were collected on a Raxis II C area detector with a Rigaku RU 300 rotating anode source. Data evaluation of thrombin−P628 complex performed with Denzo and Scalepack (*25, 26*) established a C_2 space group having cell parameters $a = 71.1$ Å, $b = 71.9$ Å, $c = 73.3$ Å, and $\beta = 100.5°$. A total of 85 433 reflections observed were merged to 20 926 unique reflections with an $R_{sym} = 0.06$ and completeness of 98.1% to 2.1 Å resolution. Thrombin−P798 complex was also crystallized in the C_2 space group having cell parameters $a = 70.8$ Å, $b = 72.0$ Å, $c = 72.9$ Å, and $\beta = 100.2°$. A total of 70 010 reflections observed were merged to 20 426 unique reflections with an $R_{sym} = 0.05$ and completeness of 95.8% to 2.1 Å resolution. Both crystals contained one complex molecule per asymmetric unit.

Structure Determination and Refinement. A thrombin molecule from the thrombin−hirutonin-2 complex (*27*) (PDB code 1ihs) was used as a model in the structural determination of thrombin−P628 and −P798 complexes. Program O version 5.10 (*28*) and X-plor 3.8 (*29*) were used in model building and in the refinement, respectively. Appropriate entries were added to the dictionaries of both programs to accommodate the nonstandard groups of the inhibitors. Rigid-body refinement of the thrombin model followed by minimization reduced the *R* facotr to 0.32 for both complexes.

The $3F_0 - 2F_c$ and difference maps calculated for thrombin at this stage showed clearly the inhibitors. They were modeled into these maps, except for D-Glu^{H65}. One hundred cycles of energy minimization were followed by molecular dynamics refinement with slow cooling from 1500 to 300 K, and the cycle was completed by another 100 cycles of energy minimization. The individual *B* factors were refined in 20 cycles of *B* factor refinement. Solvent molecules were added to the model. Several cycles of the refinement were performed, followed by model refitting to $3F_o - 2F_c$, $F_o - F_c$, and the omit maps. The final structure includes A-chain Asp^{1A}-Lys^{14A} and B-chain Ile^{16}-Glu^{146} and Gly^{150}-Phe^{245} of thrombin and all residues of P628 except D-Glu^{H65} or all residues of P798 except Cha^{H64}-(D-Glu^{H65}). The thrombin−P628 and −P798 complexes also include 142 and 160 water molecules, respectively. The final *R* factor for the reflections within the 8−2.1 Å resolution range was 0.192 (*R*-free = 24.0%) and 0.187 (*R*-free = 23.3%) with $I > \sigma(I)$ for the thrombin−P628 and −P798 complexes, respectively. The rms deviation of the bond length was 0.009 and 0.008 Å for the thrombin−P628 and −P798 complexes, respectively. The rms deviation of the bond angle was 1.72° and 1.70° for the thrombin−P628 and −P798 complexes, respectively. The backbone dihedral angles (ϕ and ψ) of the inhibitors and the thrombin residues were in the allowed region of the Ramachandra plot except Ala^{H63} of P628.

RESULTS AND DISCUSSION

P1′ Residue of the Bivalent Inhibitors. A series of bivalent thrombin inhibitors Bbs-Arg-(D-Pip)-Xaa-Gly-Gly-Gly-βAla-Asp-Tyr-Glu-Pro-Ile-Pro-Glu-Glu-Ala-Cha-(D-Glu)-OH were synthesized by incorporating various nonpolar amino acids at the P1′ residue Xaa, where Gly was used as a reference amino acid ($K_i = 2.4 \times 10^{-11}$ M) (Table 1). As reported in Methyl Scan (*21*), the P1′ residue Ala improved the affinity 20-fold with a K_i value of $(1.2 \pm 0.4) \times 10^{-12}$ M (P1004), whereas D-Ala improved the affinity 6-fold with a K_i value of $(4.2 \pm 0.5) \times 10^{-12}$ M (P1005), suggesting preference for L-amino acid at the P1′ residue. Simultaneous incorporation of D- and L-Ala, i.e., αAib, did not improve the affinity any further, with a K_i value of $(2.4 \pm 0.5) \times 10^{-12}$ M (P1373), possibly due to the conformational constraint of the αAib backbone (*30*). Introduction of a γ-methyl group, i.e., substitution of the P1′ residue Ala with αAbu, improved the affinity 2-fold with a K_i value of $(6.3 \pm 0.5) \times 10^{-13}$ M (P1378). Introduction of a δ-methyl group by substituting

Table 1: Inhibition Constant of Bivalent Thrombin Inhibitors Bbs-Arg-(D-Pip)-Xaa-Gly-Gly-Gly-βAla-Asp-Tyr-Glu-Pro-Ile-Pro-Glu-Glu-Ala-Cha-(D-Glu)-OH

ID no.	Xaa	K_i (pM)	ID no.	Xaa	K_i (pM)
P836	Gly	24 ± 5			
P1004	Ala	1.2 ± 0.4	P1005	D-Ala	4.2 ± 0.5
P1373	αAib	2.4 ± 0.5			
P1378	αAbu	0.63 ± 0.05	P1379	D-αAbu	4.3 ± 0.4
P1376	Nva	0.24 ± 0.05	P1375	D-Nva	5.1 ± 0.4
P1377	Nle	0.082 ± 0.006	P1374	D-Nle	5.3 ± 0.3
P1387	Met	0.11 ± 0.03	P1395	D-Met	4.8 ± 0.3
P1381	Val	0.84 ± 0.05	P1380	D-Val	3.7 ± 0.4
P1420	Tbg	1.1 ± 0.3	P1421	D-Tbg	5.8 ± 0.4
P1438	Pen	1.5 ± 0.4	P1439	D-Pen	6.8 ± 0.5
P1383	Ile	0.14 ± 0.04	P1384	D-Ile	4.3 ± 0.3
P1382	Leu	0.12 ± 0.04	P1385	D-Leu	2.6 ± 0.5
P1399	Chg	0.35 ± 0.5			
P1388	Cha	0.12 ± 0.04	P1396	D-Cha	7.2 ± 0.3
P1397	Phg	3.1 ± 0.4	P1398	D-Phg	7.8 ± 0.5
P1386	Phe	0.51 ± 0.05	P1394	D-Phe	3.4 ± 0.3
P1400	Hph	0.18 ± 0.05	P1441	D-Hph	2.8 ± 0.5
P1391	Trp	630 ± 30	P1443	D-Trp	820 ± 50
P1389	His	0.91 ± 0.04	P1442	D-His	2.1 ± 0.3
P1392	Thi	0.051 ± 0.004	P1393	D-Thi	2.8 ± 0.4

the P1′ residue αAbu with Nva further improved the affinity 2.5-fold with a K_i value of $(2.4 \pm 0.5) \times 10^{-13}$ M (P1376). Addition of an ϵ-methyl group by substituting the P1′ residue Nva with Nle further improved the affinity 3-fold with a K_i value of $(8.2 \pm 0.6) \times 10^{-14}$ M (P1377). Thus, moderate but steady 2−3-fold improvement of the affinity was observed when linear alkyl side chains were introduced at the P1′ residue, except 20-fold drastic improvement when the methyl side chain of Ala was introduced. On the other hand, the corresponding D-amino acid substitutions with D-αAbu, D-Nva, and D-Nle showed no improvement. These linear alkyl side chains of D-amino acids might be exposed to the solvent or have little interaction with thrombin. Incorporation of Met, which is homologous to Nle, at the P1′ residue showed an affinity, with a K_i value of $(1.1 \pm 0.3) \times 10^{-13}$ M (P1387), similar to that ($K_i = (8.2 \pm 0.6) \times 10^{-14}$ M) of Nle (P1377).

Branched analogues of αAbu showed little effect on the affinity of the inhibitors, i.e., Val, Tbg, and Pen, with K_i values of $(8.4 \pm 0.5) \times 10^{-13}$ (P1381), $(1.1 \pm 0.3) \times 10^{-12}$ (P1420), and $(1.5 \pm 0.4) \times 10^{-12}$ (P1438) M, respectively, compared to $(6.3 \pm 0.5) \times 10^{-13}$ M of αAbu (P1378). On the other hand, branched analogues of Nva showed weak improvements with K_i values of $(1.4 \pm 0.4) \times 10^{-13}$ M with Ile (branching at the Cβ atom) (P1383) and of $(1.2 \pm 0.4) \times 10^{-13}$ M with Leu (branching at the Cγ atom) (P1382) compared to $(2.4 \pm 0.5) \times 10^{-13}$ M of Nva (P1376). Chg and Cha are the bulky cyclic nonpolar side chains with reduced conformational flexibility. The K_i values of these analogues were $(3.5 \pm 0.5) \times 10^{-13}$ (P1399) and $(1.2 \pm 0.4) \times 10^{-13}$ (P1388) M for Chg and Cha, respectively, showing no improvement compared to the linear alkyl side chains. Among the linear, branched, and cyclic alkyl side chains, the inhibitor P1377 with Nle had the highest affinity. Since the amide bonds of the linker might affect the interactions of the P1′ residue with thrombin, three amide bonds in the P1377 linker Gly-Gly-Gly-βAla were eliminated by substituting with λAdod. The resulting inhibitor P628 [Bbs-Arg-(D-Pip)-Nle-λAdod-Asp-Tyr-Glu-Pro-Ile-Pro-Glu-Glu-Ala-Cha-(D-Glu)-OH] improved the affinity 2-fold to a K_i value of $(3.8 \pm 0.6) \times 10^{-14}$ M. The crystal structure of the thrombin−P628 complex is described below.

Table 2: Active Site Directed Thrombin Inhibitors Bbs-Arg-(D-Pip)-Xaa-NH_2

ID no.	Xaa	K_i (nM)	ID no.	Xaa	K_i (nM)
P972	None	180 ± 20	P898	Hph	25 ± 3
P887	Gly	550 ± 30	P899	Thi	5.2 ± 0.4
P891	Nle	25 ± 4			

The aromatic side chain was also introduced at the P1′ residue. Incorporation of Phg improved the affinity 8-fold with a K_i value of $(3.1 \pm 0.4) \times 10^{-12}$ M (P1397) compared to that with Gly (P836) ($(2.4 \pm 0.5) \times 10^{-11}$ M). The substitutions with longer aromatic side chains (Phe and Hph) improved the affinity further, i.e., $K_i = (5.1 \pm 0.5) \times 10^{-13}$ M for Phe (P1386) and $(1.8 \pm 0.5) \times 10^{-13}$ M for Hph (P1400), suggesting a deep pocket of the S1′ subsite. However, Trp was too bulky to fit at the S1′ subsite, resulting in a high K_i value of $(6.3 \pm 0.3) \times 10^{-10}$ M (P1391). The replacement of Phe with His (P1389) did not improve the affinity. However, when a His homologue (Thi) was in this position, the affinity was increased 10-fold, with $K_i = (5.1 \pm 0.4) \times 10^{-14}$ M (P1392). When the Gly-Gly-Gly-βAla linker in this compound was replaced by λAdod as in P628, the resulting inhibitor P798 [Bbs-Arg-(D-Pip)-Thi-λAdod-Asp-Tyr-Glu-Pro-Ile-Pro-Glu-Glu-Ala-Cha-(D-Glu)-OH] gained 3-fold in affinity, $K_i = (1.7 \pm 0.4) \times 10^{-14}$ M. The crystal structure of the thrombin−P798 complex is described below. All examined inhibitors with D-amino acids at the P1′ position showed a higher K_i value than that of the inhibitor with a corresponding L-amino acid (Table 1). Thus, the P1′ position clearly shows preference for L-amino acids.

P1′ Residue of the Active Site Inhibitors. The bivalent thrombin inhibitors in this paper use short 16-atom linkers. Since the 16-atom linkers are stretched along the deep cleft between the active site and the FRE (*31*), the P1′ residue is forced to be in the vicinity of the S1′ subsite. Such restriction was not present in the active site inhibitors Bbs-Arg-(D-Pip)-Xaa-NH_2 where various nonpolar amino acids were incorporated at the P1′ residue Xaa (Table 2). A reference peptide, Bbs-Arg-(D-Pip)-Gly-NH_2 (P887), showed a K_i value of $(5.5 \pm 0.3) \times 10^{-7}$ M. Bbs-Arg-(D-Pip)-NH_2 (P972), which is missing the P1′ residue, showed a 3 times lower K_i value of $(1.80 \pm 0.20) \times 10^{-7}$ M. Thus, the cost of introducing the P1′ residue Gly is 0.66 kcal/mol. This cost may be overcome by incorporating an appropriate side chain at the P1′ residue. The P1′ amino acids which improved the affinity in the bivalent inhibitors, Bbs-Arg-(D-Pip)-Xaa-Gly-Gly-Gly-βAla-Asp-Tyr-Glu-Pro-Ile-Pro-Glu-Glu-Ala-Cha-(D-Glu)-OH, also improved the affinity of the active site inhibitors Bbs-Arg-(D-Pip)-Xaa-NH_2. Nle improved the affinity of the active site inhibitor by 22-fold with a K_i value of $(2.5 \pm 0.4) \times 10^{-8}$ M (P891) compared to the 290-fold improvement in the bivalent inhibitor (P1377). Similarly, Hph improved the K_i value by 22-fold ($K_i = (2.5 \pm 0.3) \times 10^{-8}$ M) in the active site inhibitor (P898) whereas there was a 133-fold improvement in the bivalent inhibitor (P1400); Thi improved the K_i value 106-fold ($K_i = (5.2 \pm 0.4) \times 10^{-9}$ M) in the active site inhibitor (P899) compared to a 470-fold improvement in the bivalent inhibitor (P1392). The smaller improvement by Nle, Hph, and Thi in the active site inhibitors compared to those in the bivalent inhibitors may come from the larger

Table 3: Inhibition Constant of Bivalent Thrombin Inhibitors Bbs-Arg-(D-Pip)-Gly-Gly-Yaa-Gly-βAla-Asp-Tyr-Glu-Pro-Ile-Pro-Glu-Glu-Ala-Cha-(D-Glu)-OH

ID no.	Yaa	K_i (pM)	ID no.	Yaa	K_i (pM)
P836	Gly	24 ± 5			
P1054	Ala	8.7 ± 0.2	P1055	D-Ala	0.96 ± 0.03
P1068	αAib	1.4 ± 0.3			
P1056	αAbu	7.4 ± 0.3	P1346	D-αAbu	0.77 ± 0.03
P1057	Nva	9.2 ± 0.4	P1075	D-Nva	0.88 ± 0.04
P1058	Nle	8.9 ± 0.5	P1074	D-Nle	0.68 ± 0.04
P1418	Met	10.4 ± 0.5	P1419	D-Met	1.5 ± 0.5
P1061	Val	1.2 ± 0.5	P1070	D-Val	0.62 ± 0.02
P1069	Tbg	4.3 ± 0.5	P1073	D-Tbg	0.44 ± 0.04
P1431	Pen	5.6 ± 0.5	P1432	D-Pen	1.5 ± 0.5
P1059	Ile	1.9 ± 0.3	P1071	D-Ile	0.35 ± 0.5
P1060	Leu	2.2 ± 0.5	P1072	D-Leu	0.62 ± 0.03
P1341	Chg	3.2 ± 0.4			
P1424	Cha	9.6 ± 0.5	P1077	D-Cha	1.5 ± 0.5
P1340	Phg	2.8 ± 0.4	P1076	D-Phg	0.095 ± 0.006
P1339	Phe	4.5 ± 0.4	P1078	D-Phe	0.13 ± 0.05
P1345	Hph	7.2 ± 0.3	P1425	D-Hph	0.78 ± 0.05
P1344	Trp	9.8 ± 0.4	P1427	D-Trp	2.2 ± 0.5
P1343	His	6.2 ± 0.5	P1426	D-His	1.4 ± 0.4
P1342	Thi	5.1 ± 0.5	P1428	D-Thi	1.2 ± 0.4

entropy loss of the P1′ residue in the active site inhibitors than that in the bivalent inhibitors.

P3′ Residue of the Bivalent Inhibitors. The Methyl Scan of the linker showed a preference for D-amino acid at the P3′ residue; i.e., substitutions of the P3′ residue Gly by L- and D-Ala improved the affinity 3- and 25-fold, respectively (*21*). A series of bivalent thrombin inhibitors Bbs-Arg-(D-Pip)-Gly-Gly-Yaa-Gly-βAla-Asp-Tyr-Glu-Pro-Ile-Pro-Glu-Glu-Ala-Cha-(D-Glu)-OH, were synthesized by incorporating various nonpolar amino acids at the P3′ residue Yaa where Gly was used as a reference amino acid (Table 3). Inhibitors P1054, P1056, P1057, and P1058 with a linear alkyl side chain of L-amino acids (Ala, αAbu, Nva, and Nle, respectively) at the P3′ residue improved the affinity ~3-fold compared to that of the reference inhibitor P836. The inhibitors P1055, P1346, P1075, and P1074 with corresponding D-amino acids (D-Ala, D-αAbu, D-Nva, and D-Nle, respectively), on the other hand, improved the affinity of the inhibitors 25−35-fold, showing ~10-fold preference for D-amino acids over L-amino acids at the P3′ residue. Elongation of the linear alkyl side chain did not affect the affinity for both L- and D-amino acids. The inhibitors P1061, P1069, P1059, and P1060 with a branched alkyl side chain of L-amino acids (Val, Tbg, Ile, and Leu, respectively) at the P3′ residue improved the affinity 5−20-fold. The branched L-amino acids are visibly preferred over the linear alkyl L-amino acids at the P3′ position. The inhibitors P1070, P1073, P1071, and P1072 with a branched side chain of D-amino acids (D-Val, D-Tbg, D-Ile, and D-Leu, respectively) improved the affinity 40−70-fold, significantly higher than the affinity of the corresponding L-amino acids. Introduction of D-Cha with a constrained conformation of the branched alkyl side chains led to less improvement than that of other D-amino acids (P1077; $K_i = (1.5 \pm 0.5) \times 10^{-12}$ M). A similar lack of improvement was found with sulfur hetero compounds (P1419 with D-Met and P1432 with D-Pen). In addition to an alkyl side chain, aromatic groups were also introduced. The inhibitors P1340, P1339, P1345, P1343, P1344, and P1342 with aromatic L-amino acids (Phg, Phe, Hph, His, Trp, and Thi, respectively) improved the affinity 2−8-fold. The inhibitors P1076, P1078, P1425, P1426, P1427, and P1428 with corresponding D-amino acids (D-Phg, D-Phe, D-Hph, D-His, D-Trp, and D-Thi, respectively) showed better improvement with an 11−250-fold increase in affinity. This indicates a strong preference for aromatic D-amino acids, more specifically for D-Phg (P1076; $K_i = (9.5 \pm 0.6) \times 10^{-14}$ M) and D-Phe (P1078; $K_i = (1.3 \pm 0.5) \times 10^{-13}$ M) at the P3′ residue. Combining the best substitutions in P1′ and P3′, Thi and D-Phg, respectively, led to a significantly reduced affinity (P1444; $K_i = (8.6 \pm 0.5) \times 10^{-11}$ M). There seems to be a conflict in simultaneous insertion of Thi and D-Phg side chains into the S1′ and S3′ subsites, respectively, even though they are separated by a flexible Gly residue.

Structures at the Active Site. Here we report the crystal structures of human α-thrombin−P628 and −P798 complexes. The P1′ residue is Nle in P628 and Thi in P798. The structures of thrombin in these complexes are nearly identical, with an rms deviation of 0.102 for all C_α atoms. The autolysis loop Glu^{146}−Lys^{149E} is disordered, as reported for other thrombin−bivalent inhibitor complexes that crystallized in the C_2 space group (*19*, *32*, *33*). Bbs^{H1}, Arg^{H2}, and $(D\text{-Pip})^{H3}$ occupy the S3, S1, and S2 subsites of thrombin, respectively (Figure 1). The structures of these residues were well defined in the electron density maps. The S3 subsite is an aryl binding pocket surrounded by Tyr^{60A}, Trp^{60D}, Glu^{97A}, Asn^{98}, Leu^{99}, Ile^{174}, Trp^{215}, and Glu^{217}. The aromatic group of the P3 residue makes favorable stacking interactions with Trp^{215}. Replacement of the phenyl group of $D\text{-Phe}^{H1}$ by a cyclohexyl group of $D\text{-Cha}^{H1}$ leads to additional contacts with the alkyl side chains of Leu^{99} and Ile^{174} and provides increased affinity (*19*). Similarly, the p-*tert*-butyl group of Bbs^{H1} in the current inhibitors interacts with the side chains of Leu^{99} and Ile^{174}, resulting in 8-fold increased affinity as compared to a corresponding inhibitor with $D\text{-Phe}^{H1}$ (data not shown). Thus, van der Waals interactions are the key element of the molecular association at the S3 subsite. Sulfonyl oxygen atoms of Bbs^{H1} are exposed to the solvent and do not interact with thrombin, suggesting little contribution to the affinity. The Arg^{H2} side chain extends into the S1 subsite as reported in thrombin−P498 and −P500 complexes (*31*). Its guanidinium $-NH_3^+$ moiety forms a salt bridge ($d = 3.0$ Å) with the carboxylate group of Asp^{189}. The guanidinium =NH of Arg^{H2} forms a hydrogen bond ($d = 3.0$ Å) with Wat^7, which is further hydrogen-bonded ($d = 2.8$ Å) to the carbonyl oxygen of $(D\text{-Pip})^{H3}$. $(D\text{-Pip})^{H3}$ occupies the S2 subsite of thrombin and adopts a chair conformation. $(D\text{-Pip})^{H3}$, the conformation of which is the same in P498−, P500−, P628−, and P798−thrombin complexes, interacts with Ser^{214} Oγ through Wat^7. The closest carbonyl carbon of the inhibitor to the catalytic oxygen of Ser^{195} is the one of $(D\text{-Pip})^{H3}$ with a distance of ~4.5 Å, which assumes the proteolytic stability of these compounds against thrombin.

Structures at the S1′ Subsite. The specificity of the thrombin S1′ site for the small P1′ residue was experimentally confirmed by characterizing the reactivity of thrombin with natural and engineered variants of antithrombin III in which Ser^{394} at the P1′ position is substituted with other amino acids (*8*, *34*−*36*). The conformation of Lys^{60F} was used to explain the substrate specificity of the P1′ residue for small amino acids such as Gly, Ala, Val, Ser, Thr, and Asp (Figure 2) (*37*). In the thrombin−P498 complex, the Lys^{60F} is close to the main chain of the inhibitor P498 [the

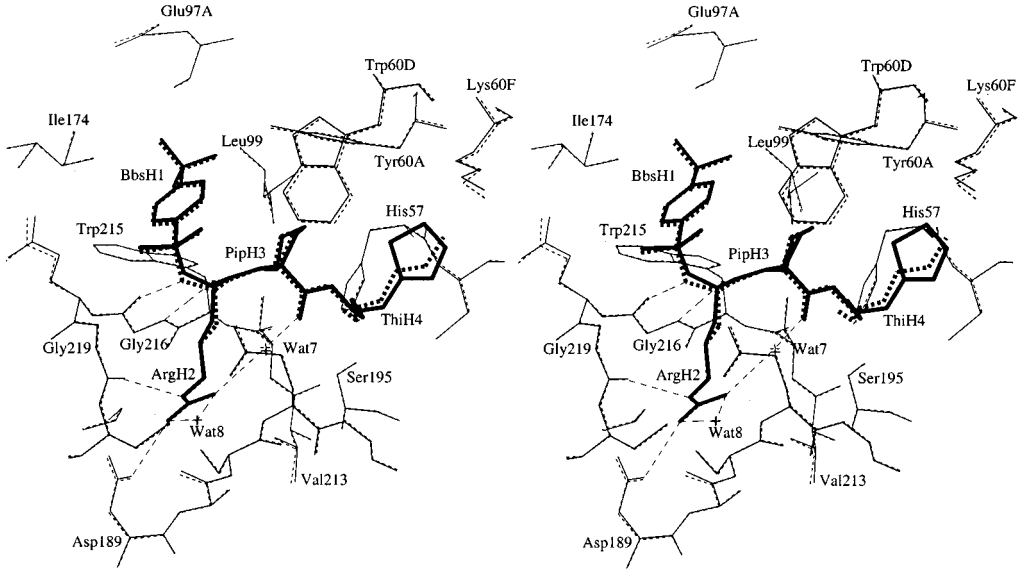

FIGURE 1: Stereoview of the crystal structures of thrombin−P628 and −P798 complexes at the thrombin active site. Thin and thick lines represent the thrombin and P798, respectively, in the thrombin−P798 complex. Thin broken and thick broken lines represent thrombin and P628, respectively, in the thrombin−P628 complex. The dashed lines represent hydrogen bonds.

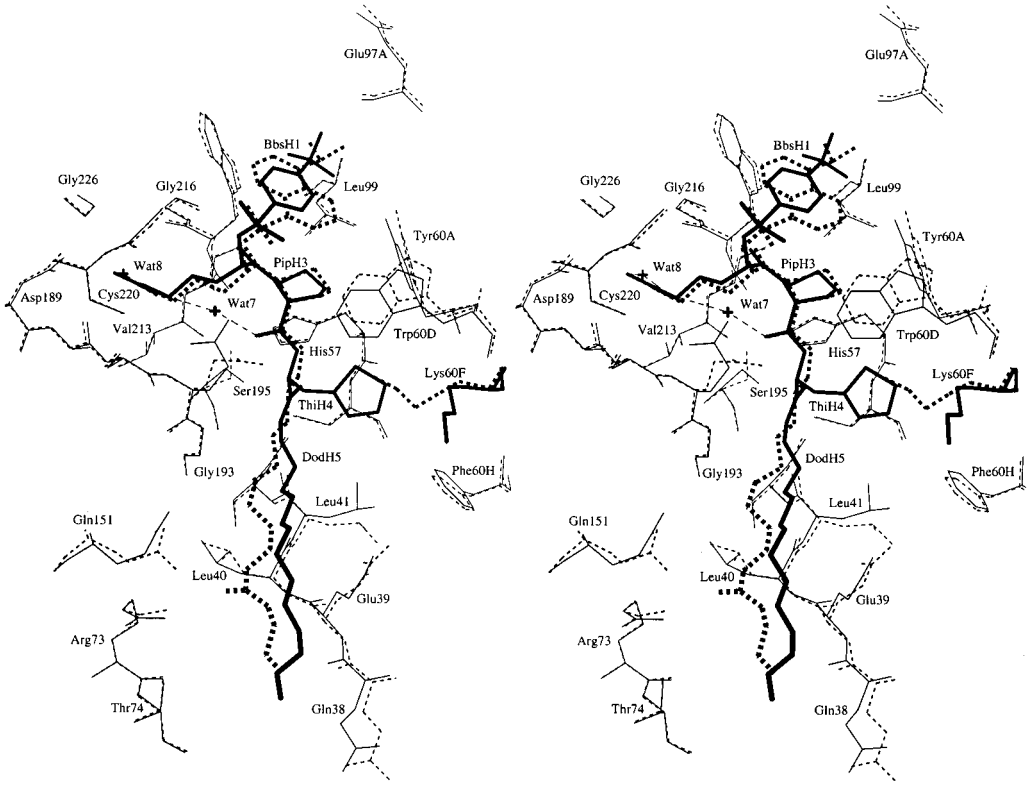

FIGURE 2: Stereoviews of the crystal structures of thrombin−bivalent inhibitor complexes at the S1′ subsite. Thin and thick lines represent the thrombin and P798, respectively, in the thrombin−P798 complex. Thin broken and thick broken lines represent thrombin and P500, respectively, in the thrombin−P500 complex for comparison. Dashed lines represent hydrogen bonds.

Nϵ of Lys^{60F} is 4.7 Å away from C$^{\alpha}$ of βAla^{H4} and is hydrogen-bonded to the amide nitrogen of βAla^{H4} through Wat^{112}]. In addition, the side chain orientations of Leu^{41}, Glu^{39}, and Leu^{33} were also different from those of the conformation observed in thrombin−P628 and −P798 complexes. However, this argument does not explain the presence of large amino acids Ile, Leu, and His in some thrombin substrates nor high affinity of the chromogenic and fluorogenic substrates, the significant portion of the affinity of which comes from its bulky nonpolar P1′ residue. The electron density of the Lys^{60F} side chain in the thrombin−P498 complex is not very well defined, suggesting flexible conformation and rather poor impediment against a bulky P1′ residue. Furthermore, another well-defined conformation of the Lys^{60F} side chain was observed by Matthews et al. (*38*) and St. Charles et al. (*39*) as well as in thrombin−P628 and −P798 complexes (Figure 2). This conformation of Lys^{60F} is well defined in the electron density with an average *B* factor of 28.9 and 33.6 Å^2 for the Lys^{60F} side chain atoms of P628 and P798 complexes, respectively. The Lys^{60F} Nϵ is hydrogen-bonded to Wat^{114} (d = 2.9 Å), which interacts with Glu^{39} through Wat^{128}. The aliphatic part of the Lys^{60F}

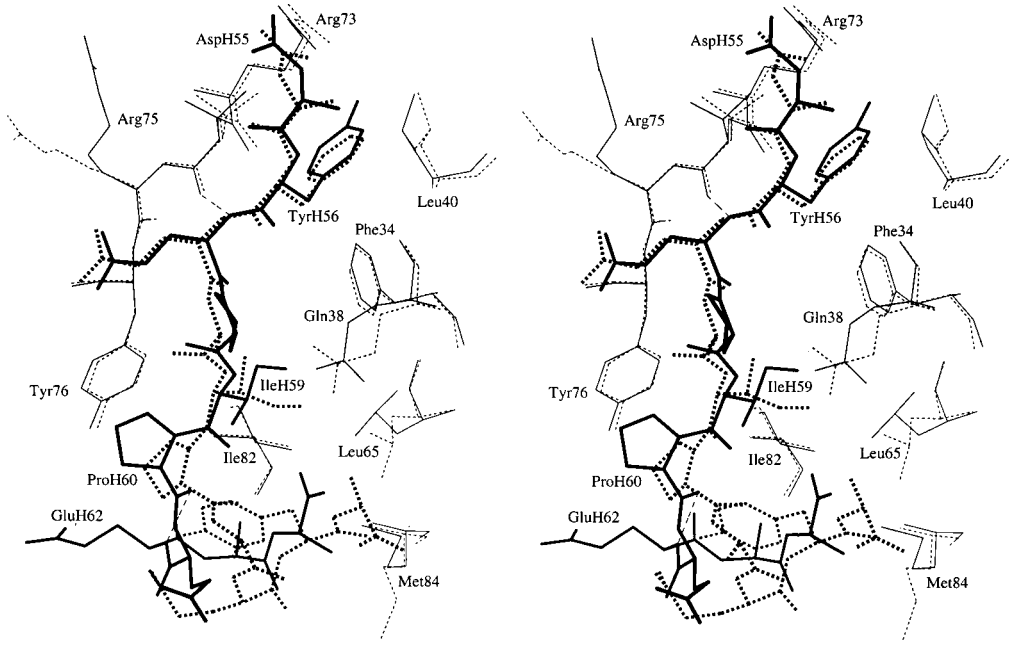

FIGURE 3: Stereoviews of the crystal structures of thrombin−bivalent inhibitor complexes at the FRE. Thin and thick lines represent the thrombin and P798, respectively, in the thrombin−P798 complex. Thin broken and thick broken lines represent thrombin and P500, respectively, in the thrombin−P500 complex for comparison. Dashed lines represent hydrogen bonds.

side chain interacts with the side chains of Leu[41], Trp[60D], and Phe[60H] through van der Waals interactions, resulting in a large and deep hydrophobic S1′ binding pocket which can accommodate the bulky nonpolar P1′ residue. Thus, the S1′ subsite is a potential nonpolar binding site that can enhance the affinity of the inhibitors and substrates. The side chain of the P1′ residue of P628 or P798 is surrounded by Leu[41], Cys[42]−Cys[58], His[57], Tyr[60A], Trp[60D], Phe[60H], and Lys[60F] as well as D-Pip[H3]. The side chain of Thi[H4] is extended into the cavity of the S1′ subsite. The thienyl ring stacks against the indole ring of Trp[60D]. The side chain of Nle[H4] is also extended into the cavity of the S1′ subsite. It forms numerous van der Waals interactions with Leu[41], Trp[60D], Phe[60H], Cys[42], and Cys[58]. The ϵ-methyl group of Nle[H4], especially, interacts with β- and γ-methylene groups of Lys[60F] (d = 3.9 and 3.8 Å, respectively).

Linker Structures. Crystal structures of thrombin−bivalent inhibitors show that the short linkers occupy the S′ subsites (*27*, *31*), whereas long linkers seem to be largely exposed to solvent (*27*). Slon-Usakiewicz et al. (*21*) reported that a linker of at least 15 atoms (including the P1′ residue) is required for optimum simultaneous bindings to the active site and the FRE. Here we used a 16-atom linker to provide some conformational flexibility. As expected, λAdod[H5] of P628 and P798 lies in the deep cleft along the S′ subsites of thrombin (Figure 2). The methylene groups of λAdod[H5] form nonpolar interactions with the side chains of Glu[39] and Glu[192]. The NH group of λAdod[H5] is hydrogen-bonded to Wat[42] (d = 3.0 Å), and the carbonyl group is hydrogen-bonded to Wat[99] (d = 2.9 Å). The carbonyl oxygen of λAdod[H5] forms an intramolecular hydrogen bond with the NH proton of Tyr[H56]. The electron density indicates that the N-terminal half of λAdod[H5] is more flexible than the C-terminal half. This moderate conformational flexibility of the linker may optimally locate the P1′ and P3′ residues into the S1′ and S3′ subsites.

FRE Structure. The structures of the FRE inhibitor segment of P628 and P798 and the thrombin FRE are essentially identical, although the side chains of Glu[H61], Glu[H62], and Cha[H64] as well as the D-Glu[H65] residue could not be identified due to the lack of electron density or to the scattered density (Figure 3). The Asp[H55] side chain forms a salt bridge (d = 2.8 Å) to Arg[73]. The electron density of Tyr[H56] is well defined. Perpendicular aromatic−aromatic stacking was observed between Tyr[H56] and Phe[34]. In addition, Met[32], Leu[40], Arg[73], Thr[74], and Gln[151] side chains form nonpolar interactions with the Tyr[H56] side chain. The hydroxy group of Tyr[H56] forms a hydrogen bond (d = 3.3 Å) with Arg[73]. The carboxyl group of Glu[H57] does not form a salt bridge; however, Glu[H57] Oϵ1 and Oϵ2 are hydrogen-bonded (d = 3.3 and 2.7 Å, respectively) to the backbone NH of Tyr[76] and Wat[49], respectively. Wat[49] is further hydrogen-bonded (d = 2.7 Å) to the backbone carbonyl oxygen of Pro[H58]. The side chains of Glu[H61] and Glu[H62] are exposed to the solvent with no interaction observed. The electron density of Ile[H59] is well defined. The average temperature factor of the entire side chain was 44.5 and 46.3 for P628− and P798−thrombin complexes, respectively. Its side chain is inserted into a hydrophobic pocket surrounded by Phe[34], Leu[65], Tyr[76], Ile[82], and Cha[H64]. The side chain of Ile[H59] adopts a conformation with $\chi_1 = -66°$ pointing $^{\delta}CH_3$ of Ile[H59] toward Arg[67] different from that ($\chi_1 = 58°$) in the hirudin[66−65] FRE inhibitor segment of hirutonin-2 (*27*). The side chains of Glu[38], Glu[39], Leu[41], Leu[65], and Met[84] were also in a different orientation (Figure 3). The Pro[H60] side chain has van der Waals interactions with Tyr[76]. The residues Glu[H61]-Glu[H62]-Ala[H63] form a 3_{10} helical turn which is stabilized by a hydrogen bond between the carbonyl oxygen of Pro[H60] and the NH proton of Ala[H63], and nonpolar interactions of the Ala[H63] side chain with Pro[H60] and Ile[H59] side chains. This turn brings Cha[H64] back to the binding pocket of Ile[H59]; however, we did not observe any clear electron density in Cha[H64] and (D-Glu)[H65] residues, suggesting their conformations are flexible.

CONCLUSIONS

The linker of bivalent thrombin inhibitors was successfully designed to interact with thrombin S′ subsites, resulting in a design of trivalent thrombin inhibitors. Among the trivalent inhibitors with a various nonpolar P1′ or P3′ residue, incorporation of aromatic D-amino acids at the P3′ residue improved the affinity ~200-fold to a K_i value of $(9.5 \pm 0.6) \times 10^{-14}$ M with D-Phg and $(1.3 \pm 0.5) \times 10^{-13}$ M with D-Phe. Incorporation of Nle and Thi at the P1′ residue also improved the affinity to a K_i value of $(3.8 \pm 0.6) \times 10^{-14}$ or $(1.7 \pm 0.4) \times 10^{-14}$ M, respectively. Crystal structures of two of the thrombin−inhibitor complexes revealed that incorporation of Nle or Thi accompanies a large conformational change of the Lys^{60F} side chain and creates a deep and large nonpolar S1′ subsite. This new S1′ subsite accepts a large nonpolar P1′ residue to improve the affinity of ligands by 2 orders of magnitude. Thus, the design of P1′ and P3′ residues converted the hirudin-based bivalent inhibitors into trivalent inhibitors, and improved the affinity to the level of natural hirudin ($K_i = 2.2 \times 10^{-14}$ M) with molecules that are one-third the size of hirudin.

ACKNOWLEDGMENT

We thank Drs. Enrico Purisima and Traian Sulea for useful discussion. We also thank Jean Lefebvre for technical assistance.

REFERENCES

1. Laudano, A. P., Cottrell, B. A., and Doolittle, R. F. (1983) *Ann. N. Y. Acad. Sci. 27*, 315−329.
2. Vu, T.-K. H., Hung, D. T., Wheaton, V. I., and Coughlin, S. R. (1991) *Cell 64*, 1057−1068.
3. Schechter, I., and Berger, A. (1967) *Biochem. Biophys. Res. Commun. 27*, 157−162.
4. Bode, W., Mayr, I., Baumann, U., Huber, R., Stone, S. R., and Hofsteenge, J. (1989) *EMBO J. 8*, 3467−3475.
5. Blombäck, B., Blombäck, M., Hessel, B., and Iwanaga, S. (1967) *Nature 215*, 1445−1448.
6. Le Bonniec, B. F., Myles, T., Johnson, T., Knight, C. G., Tapparelli, C., and Stone, S. R. (1996) *Biochemistry 35*, 7114−7122.
7. Martin, P. D., Robertson, W., Turk, D., Huber, R., Bode, W., and Edwards, B. F. P. (1992) *J. Biol. Chem. 267*, 7911−7920.
8. Rezaie, A. R., and Olson S. T. (1997) *Biochemistry 36*, 1026−1033.
9. Maraganore, J. M., Bourdon, P., Jablonsky, J., Ramachandran, K. l., and Fenton, J. W. II (1990) *Biochemistry 29*, 7095−7101.
10. DiMaio, J., Gibbs, B., Munn, D., Lefebvre, J., Ni, F., and Konishi, Y. (1990) *J. Biol. Chem. 265*, 21698−21703.
11. Bourdon, P., Jablonski, J.-A., Chao, B. H., and Maraganore, J. M. (1991) *FEBS Lett. 294*, 163−166.
12. DiMaio, J., Ni, F., Gibbs, B., and Konishi, Y. (1991) *FEBS Lett. 282*, 47−52.
13. DiMaio, J., Gibbs, B., Lefebvre, J., Konishi, Y., Munn, D., Yue, S.-Y., and Hornberger, W. (1992) *J. Med. Chem. 35*, 3331−3341.
14. Kline, T., Hammond, C., Bourdon, P., and Maraganore, J. M. (1991) *Biochem. Biophys. Res. Commun. 177*, 1049−1055.
15. Krishnan, R., Tulinsky, A., Vlasuk, G. P., Pearson, D., Vallar, P., Bergum, P., Brunck, T. K., and Ripka, W. C. (1996) *Protein Sci. 5*, 422−433.
16. Lombardi, A., Nastri, F., Morte, R. D., Rossi, A., De Rosa, A., Staiano, N., Pedone, C., and Pavone, V. (1996) *J. Med. Chem. 39*, 2008−2017.
17. Skordalakes, E., Elgendy, S., Goodwin, C. A., Green, D., Scully, M. F., Kakkar, V. V., Freyssinet, J.-M., Dodson, G., and Deadman, J. J. (1998) *Biochemistry 37*, 14420−14427.
18. Lombardi, A., De Simone, G., Nastri, F., Galdiero, S., Morte, R. D., Staiano, N., Pedone, C., Bolognesi, M., and Pavone, V. (1999) *Protein Sci. 8*, 91−95.
19. Rehse, P. H., Steinmetzer, T., Li, Y., Konishi, Y., and Cygler, M. (1995) *Biochemistry 34*, 11537−11544.
20. Tsuda, Y., Cygler, M., Gibbs, B. F., Pedyczak, A., Féthière, J., Yue, S.-Y., and Konishi, Y. (1994) *Biochemistry 33*, 14443−14451.
21. Slon-Usakiewicz, J. J, Purisima, E., Tsuda, Y., Sulea, T., Pedyczak, A., Féthière, J., Cygler, M., and Konishi, Y. (1997) *Biochemistry 36*, 13494−13502.
22. Szewczuk, Z., Gibbs, B. F., Yue, S.-Y., Purisima, E., Zdanow, A., Cygler, M., and Konishi, Y. (1993) *Biochemistry 32*, 3396−3404.
23. Szewczuk, Z., Gibbs, B. F., Yue, S.-Y., Purisima, E., and Konishi, Y. (1992) *Biochemistry 31*, 9132−9140.
24. Segel, I. H. (1975) *Enzyme Kinetics: Behawior and Analysis of Rapid Equilibrium and Steady-State Enzyme Systems*, pp 100−160, John Wiley & Sons, New York.
25. Otwinowski, Z. (1993) *Proceedings of the CCP4 Study Weekend: "Data Collection and Processing"*, Jan29−30, 1993, pp 56−62, SERC Daresbury Laboratory, England (compiled by Sawyer, L., Isaacs, N., and Bailey, S.).
26. Minor, W. (1993) XDISPLAY Program, Purdue University.
27. Zdanov, A., Wu, S., DiMaio, J., Konishi, Y., Li, Y., Wu, X., Edwards, B. F. P., Martin, P. D., and Cygler, M. (1993) *Proteins 17*, 252−265.
28. Jones, T. A., Zhou, J. Y., Cowan, S. W., and Kjeldgaard, M. (1991) *Acta Crstallogr. A47*, 110−119.
29. Brunger, A. T. (1993) X-plor version 3.1, Yale University, New Haven, CT.
30. Okuyama, K., and Ohuchi, S. (1996) *Biopolymers 40*, 85−103.
31. Féthière, J., Tsuda, Y., Coulombe, R., Konishi, Y., and Cygler, M. (1996) *Protein Sci. 5*, 1174−1183.
32. Skrzypczak-Jankun, E., Carperos, V. E., Ravichandran, K. G., Tulinsky, A., Westbrook, M., and Maraganore, J. M. (1991) *J. Mol. Biol. 221*, 1379−1393.
33. Qiu, X., Padmanabhan, K. P., Carperos, V. E., Tulinsky, A., Kline, T., Maraganore, J. M., and Fenton, J. W., II (1992) *Biochemistry 31*, 11689−11697.
34. Stephens, A. W., Siddiqui, A., and Hirsh, C. H. W. (1988) *J. Biol. Chem. 263*, 3639−3645.
35. Theunissen, H. J. M., Dijiikema, R., Grootenhuis, P. D. J., Swinkels, J. C., DePoorter, T. L., Carati, P., and Visser, A. (1993) *J. Biol. Chem. 268*, 9035−9040.
36. Wnendt, S., Janocha, E., Steffens, G. J., and Strassburger, W. (1997) *Protein Eng. 10*, 169−173.
37. Stubbs, M. T., and Bode, W. (1993) *Thrombin Res. 69*, 1−58.
38. Matthews, J. H., Krishnan, R., Costanzo, M. J., Maryanoff, B. E., and Tulinsky, A. (1996) *Biophys. J. 71*, 2830−2839.
39. St. Charles, R., Matthews, J. H., Zhang, E., and Tulinsky, A. (1999) *J. Med. Chem. 42*, 1376−1383.

BI992419B